Experimental Investigation of Oscillations in Flows Over Shallow Cavities

Virendra Sarohia*
California Institute of Technology, Pasadena, Calif.

Laminar axisymmetric flows over shallow cavities at low subsonic speeds were experimentally investigated. The results indicate that the cavity depth has little effect on oscillations in shallow cavities, except when the depth is of the order of the thickness of the cavity shear flow. For such cavity configurations, measurements indicate a strong stabilizing effect of depth on laminar cavity shear layer. Results of motion picture and hot-wire surveys of the cavity shear layer show that, close to the downstream cavity corner, large lateral motion of the shear layer occurs, which results in a periodic shedding of vortices at a frequency of cavity oscillation. Mean velocity measurements show growth rates as high as $d\theta/dx \simeq 0.022$, where θ is the shear layer momentum thickness and x is the streamwise coordinate. These are attributed to strong imposed velocity fluctuations on the flow, by the oscillating cavity system. Phase measurements indicate that the disturbances propagate at a constant phase speed through the cavity shear layer. The wavelength of the propagating disturbance bears an approximate integral relation to cavity width, in each mode of cavity oscillation given by $b \simeq \lambda(n + 1/2)$, where b is the cavity width, λ the wavelength of the propagating disturbance, and n is an integer, which takes values 0, 1, 2, ... etc., depending upon the mode of oscillation.

Nomenclature

b = cavity width (cavity length)
d = cavity depth
f = frequency in Hz
ℓ = nose length of the model
n = an integer
u' = velocity in direction x
U = mean velocity in direction x
U_e = mean velocity at the upstream cavity corner
U_c = convective speed of the disturbances in the cavity shear layer
U_∞ = freestream velocity in front of the model
x = streamwise coordinate
y = transverse coordinate
$\delta(x)$ = shear-layer thickness at x
$\theta(x)$ = shear-layer momentum thickness at x
λ = disturbance wavelength
ν = kinematic viscosity
ψ = phase angle by which the phase at a given location lags behind $x = 0$
$\frac{fb}{U_e}, \frac{f\theta}{U_e}, \frac{f\delta}{U_e}$ = nondimensional frequencies
$Re_{\delta 0} = \frac{U_e \delta_0}{\nu}$, Reynold number based on δ_0
$Re_{\theta 0} = \frac{U_e \theta_0}{\nu}$, Reynold number based on θ_0
$(\ )_{\min}$ = corresponds to the conditions for onset of cavity oscillations

I. Introduction

THE problem of fluid flow (gases or liquids) over cavities on solid surfaces has gained renewed significance. For example, uncovered cavities on flight vehicles are necessary to house optical instruments. Other applications occur in the transonic wind tunnel where slotted walls are used, in continuous laser cavities, and even in cavities of ship hulls. Flow over cavities is of interest, because the presence of cavities changes the drag and heat transfer and may cause intense periodic oscillations, which in turn may lead to severe buffeting of the aerodynamic structure and production of sound.

Periodic oscillations in cavities have been observed over a large range of Mach numbers and Reynolds numbers, with both laminar and turbulent boundary layers and over a wide range of length-to-depth ratios. In general, cavities are divided into open and closed cavities as defined by Charwat et al.[1] Open cavities refer to flow over cavities where the boundary layer separates at the upstream corner and reattaches near the downstream corner. Cavities are closed when the separated layer reattaches at the cavity bottom and again separates ahead of the downstream wall. At supersonic speeds and for a turbulent layer, the dividing line between open and closed cavities was found to be $b/d \simeq 11$ by Charwat et al. Present experiments at low subsonic speeds with laminar separation show a demarcation line between an open and a closed cavity to be approximated by $b/d \simeq 7$-8.

Open cavities may further be divided into shallow and deep cavities. On the basis of previous experiments,[2,3] the oscillations in deep cavities are in fundamental acoustic depth modes. Deep cavities act as resonators and the shear layer above the cavity provides a forcing mechanism. Resonant oscillations are established under certain flow conditions, corresponding to natural acoustic depth modes of the cavities.

In contrast to deep cavities, present experiments of flow over shallow cavities at low subsonic speed show that the phenomenon of cavity oscillations is not one of the standing longitudinal acoustic waves but one of propagating disturbances which get amplified through the shear layer. The important length scale, therefore, in shallow cavity flows, is the width b of the cavity. On the basis of past experiments,[2-4] a very rough division between shallow and deep cavities is $b/d \simeq 1$. For $b/d > 1$ the cavities may be considered shallow, and for $b/d < 1$ the cavities may be considered deep.

Previous work on cavity oscillations has been mainly experimental. Because of the practical importance of oscillations in bomb bays, experiments were performed at Boeing,[5] Douglas,[6] and at the Royal Aircraft Establishment.[7] The first experiments covering a wide range of

Presented as Paper 76-182 at the AIAA 14th Aerospace Sciences Meeting, Washington, D.C., Jan. 26-28, 1976; submitted Oct. 6, 1976; revision received April 15, 1977.

Index categories: Jets, Wakes, and Viscid-Inviscid Flow Interactions; Nonsteady Aerodynamics; Aeroacoustics.

*Senior Scientist, Energy and Materials Research Section, Jet Propulsion Laboratory. Member AIAA.

geometrical and flow parameters were performed by Karamchet.[8] Further extensive work was performed by East,[2] Heller et al.,[9] McGregor and White,[10] Plumblee et al.,[3] Rossiter,[7,11] and others.[12-15]

Karamcheti studied the acoustic field of two-dimensional shallow cavities in the range of Mach numbers from 0.25 to 1.5 by schlieren and interferometric observations. Karamcheti noticed that, for a fixed freestream Mach number and depth, there exists a minimum width below which no sound emission is noticed. For a fixed cavity, experimental results further showed a minimum Mach number below which no sound emission was noticed. Under a nonoscillating cavity configuration, schlieren and spark shadowgraph pictures showed that the shear layer bridges the cavities without strong interaction with the downstream corner. No detailed study of the aerodynamic and geometric conditions for the onset of cavity oscillations was undertaken.

The effects of Mach number on nondimensional frequency fb/U_e have been studied by many investigators for both laminar and turbulent boundary layers. On the basis of high-speed shadowgraphs of cavity oscillations, Rossiter[11] speculated that periodic vortices are shed at the upstream corner in sympathy with the pressure oscillation produced by interaction of the vortices with the downstream corner. Based on this idea Rossiter derived a formula for the oscillation frequency. Heller et al.[9] studied shallow cavities over a wide range of Mach numbers and correlated a great many experimental results with Rossiter's formula. In Rossiter's formulations of cavity oscillation frequency, the vortices shed from the upstream cavity corner are assumed to convect at a constant phase velocity through the shear layer, resulting in a linear phase distribution. It is further assumed that the phase velocity of these vortices is independent of the cavity geometry and flow configuration. Rossiter's formula does not shed any light on the possible mode or modes in which the cavity is most likely to oscillate. Unfortunately, no systematic measurements of cavity shear layer have been made in the past to verify Rossiter's assumptions.

For a given flow, the prerequisite of a minimum width for the onset of cavity oscillations strongly suggests that the mechanism of cavity oscillations depends upon the stability characteristics of the shear layer. Woolley[16] and Karamcheti extended their stability analysis of nonparallel jets for edge-tone generation to explain the main features of cavity oscillations qualitatively. Their measurements[17-19] of edge-tone flowfield indicated that the phase and propagation speed of the disturbances in the jet do not agree with the linearized stability theory of the incompressible two-dimensional parallel jet. According to the stability theory of nonparallel shear flows, the stability characteristic of the flow is a function of local quantities, viz., thickness of the shear layer, mean velocity profile, etc., which result in different amplification rates as a disturbance of fixed frequency propagates downstream through the flow. This explains their measurements of edge-tone flowfield in which, according to them, a nonlinear distribution of the phase and convective speed of the disturbances occurs. They speculated that a similar behavior would occur in cavity flows and extended their results accordingly. On the basis of stability of almost parallel shear flow, they concluded that the frequency of cavity oscillations is the one which received the maximum total integrated amplification through the shear layer. Their theory does not take into consideration the presence of the downstream corner that this study indicates to be the key factor in inducing self-sustained oscillations in the cavity shear layer. Present experiments further show that the presence of a back face, in fact, results in an integral relation between the wavelength of the propagating disturbance and the cavity width, in each mode of cavity operation.

It was therefore felt that a detailed measurement of the cavity shear layer was necessary for better understanding of the mechanism. Flow visualization and measurements of the cavity shear layer, from which phase distribution, phase velocity of the propagating disturbance, etc., can be determined, would be of great help in understanding the phenomenon of cavity oscillations.

II. Experimental Arrangement

Model and Wind Tunnel

In the present study, three axisymmetric models were employed with outer diameter D of 1, 2, and 6 in. These models had an arrangement for variation of depth d in steps and continuously varying with b. The 1-in.-diam model with a hemispherical nose was used mostly for preliminary experimental work. The main quantitative work was done on the 2-in. and 6-in. models. The 2-in. diam model had ojive-shape noses, whereas an elliptic nose was used for the 6-in. model. For all these models, the boundary layer at separation was laminar. The details of these models are given in Fig. 1.

The 2-in. model was made of aluminum with step depths d of 0.875, 0.5, 0.25, 0.125, and 0.05 in. The width b could be

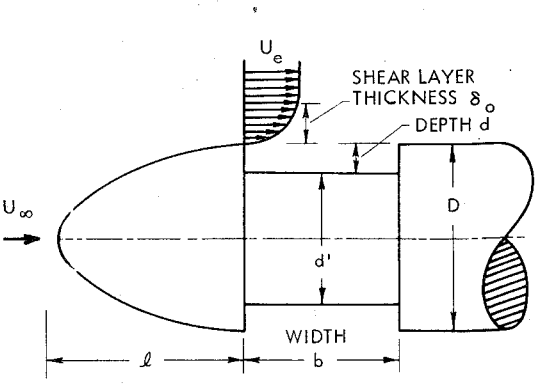

D = 1.0", 2.0" AND 6.0"
b AND d ARE VARIABLE
U_e: 0-80 ft/sec
Re_D: $2 \times 10^4 - 10^5$ (LAMINAR BOUNDARY LAYER AT SEPARATION)
FREE STREAM TURBULENCE
AT 50 ft/sec ~ 0.3% $\sqrt{u'^2}/U_\infty$

NOSE SHAPE
D = 1.0" HEMISPHERICAL NOSE
D = 2.0" I OGIVE WITH $\ell/D = 0.6$
II OGIVE WITH $\ell/D = 1.12$
III OGIVE WITH $\ell/D = 2.12$
D = 6.0" ELLIPSOID WITH RATIO OF MAJOR TO MINOR AXIS = 3.

Fig. 1 Model of cavity oscillations with pertinent nomenclature.

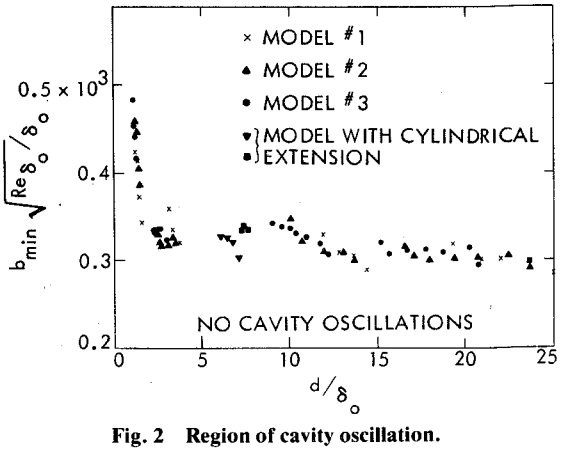

Fig. 2 Region of cavity oscillation.

varied continuously from 0.0. to 2.5 in. The accuracy of measuring width b was ± 0.002 in. This model had a family of three ogive nose shapes with ℓ/D of 0.6, 1.12, and 2.12 in. To analyze cavity flow, a hot-wire probe was inserted from outside into the shear layer. The probe could be moved with ± 0.001-in. accuracy across and along the shear layer. This model had a provision for injecting smoke from inside the cavity. The flow around it was investigated in a 6-in free jet tunnel.

The second model tested was of 6-in. diam D. This model was tested in 2×2 ft. rectangular section, open circuit wind tunnel. It had a semiellipsoidal head with a major to minor axis ratio of 3. Cavity depths d could be set at 0.5, 1, 1.5, and 2 in. The model had provision for insertion of a hot-wire from inside the cavity. This probe could be moved along and across the axis of the model. Another hot wire probe was brought from the top of the wind tunnel and could be moved very precisely up and down and along the axis of the model. The two hot-wire probes could be moved circumferentially relative to each other to check the axisymmetry of the cavity flow.

Instrumentation

Constant temperature hot-wire anemometry was extensively used in measuring both mean and fluctuating streamwise velocity components. The output of the hot-wire was fed to a wave analyzer to analyze the frequency contents of the cavity flow. Electronic sweeping was used and the output of the wave-analyzer was fed to a rms voltmeter. The mean square output from the rms meter (available as d.c.) was fed to an x-y plotter to measure the relative amplitude of the frequency content in the hot-wire signal. For phase angle and phase velocity measurements, the output of the two hot wires was analyzed on an SAI Correlation and Probability Analyzer. The output of the correlation measurement was displayed on an oscilloscope or plotted on an x-y plotter.

Flow Visualization

Flow around the cavity was visualized by injecting smoke from inside the cavity. This was done at various locations, viz., close to the upstream and downstream corner, just after the downstream corner, etc., to study the details of flow around the cavity. The model was lighted from above. Both still and motion pictures of the cavity flow were taken.

III. Experimental Results

Minimum Width for Oscillating to Occur

It has been observed experimentally for flow over cavities that, for given flow conditions, there exists a minimum width $b_{\min}$ below which no oscillation occur. Also, no cavity oscillations occur below a minimum velocity $U_{e\min}$ for a given cavity geometry and boundary-layer thickness at δ_0 at separation.

A detailed investigation of the effect of flow and cavity geometry on the onset of the cavity oscillations was undertaken on the 2-in.-diam model. A family of three ogive nose shapes (with $\ell/D = 0.6$, 1.12, and 2.12) were employed. For a fixed nose shape and depth d, edge velocity U_e was determined for various widths b at which the cavity began to oscillate. For the same nose shape, the above experiment was repeated with five different depths. This gave one set of experimental data. Two other similar sets of data were obtained for the other two nose shapes. A total of 90 data points of known U_e, δ, b, d, and f at which oscillations began were obtained. When the data were nondimensionalized and plotted as a nondimensional width $(b_{\min}/\delta_0)\ (U_e\delta_0/\nu)^{1/2}$ against the nondimensional depth d/δ_0, all the experimental results fell on a single curve. Figure 2 shows the results of the experiments. No cavity oscillations occur below these points. It is clear from these results that the depth has little effect on the nondimensional width $(b_{\min}/\delta_0)\ (U_e\delta_0/\nu)^{1/2}$ when depth $d/\delta_0 > 2$. There is a sharp increase in $(b_{\min}/\delta_0)\ (Re\delta_0)^{1/2}$ when $d/\delta_0 \sim O(1)$.

To investigate the effect of any pressure gradient before separation, the length of the ogive nose was varied by means of two cylindrical extensions. Relatively thick boundary layers, which were laminar at separation, were obtained. The minimum width for a particular depth was determined again by changing edge velocity U_e. These results are also shown in Fig. 2.

Nondimensional Frequency of Cavity Oscillations

For an axisymmetric model, the nondimensional frequency fb/U_∞ for low subsonic flows can be expressed as

$$\frac{fb}{U_\infty} = F' \times \left(\frac{U_e\delta_0}{\nu}, \frac{b}{\delta_0}, \frac{d}{\delta_0}, \text{ mean velocity profile at separation, etc.} \right)$$

Experimental results (shown later) indicate that nondimensional frequency is independent of ℓ/D and the most important parameters defining cavity oscillations are U_e and δ_0 instead of U_∞, D, and ℓ. Therefore, one can write nondimensional frequency fb/U_e as a function

$$\frac{fb}{U_\infty} = F \times \left(\frac{U_\infty \ell}{\nu}, \frac{b}{D}, \frac{d'}{D}, \frac{\ell}{D}, \text{ mean velocity profile at separation, etc.} \right)$$

To study the dependence of nondimensional frequency on Reynolds number $Re\delta_0 = U_e\delta_0/\nu$, depth d/δ_0 and width b/δ_0, each of them was varied separately, keeping others constant.

Effect of Width

Figure 3 shows the effect of width on cavity oscillations at Reynolds number $Re\delta_0 = 2.86 \times 10^3$ and depth $d/\delta_0 = 10$ where nondimensional frequency fb/U_e is plotted against nondimensional width b/δ_0. No cavity oscillations occurred below $b/\delta_0 = 5.25$, which represents the minimum width $(b/\delta_0)_{\min}$. First mode fluctuations occurred at a nondimensional frequency of about 0.6. There was a slow increase in nondimensional frequency as b/δ_0 increased. As the critical value of $b/\delta_0 = 8.15$ was reached, oscillations jumped to a higher mode. At this width, two modes occurred alternately. The two modes never occurred simultaneously. Under certain flow conditions, switching between the two modes was audible. The second mode of cavity oscillations occurred at a nondimensional frequency of approximately 0.95. As the width b/δ_0 was increased slightly beyond the critical value of 8.15, the first mode disappeared and the flow began to oscillate in the second mode of cavity oscillation. As the width was

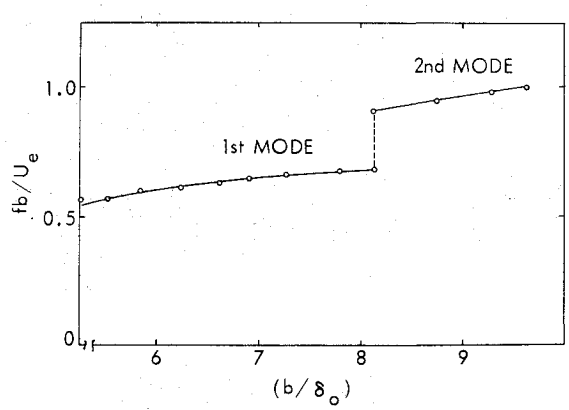

Fig. 3 Effect of width on nondimensional frequency at $Re\delta_0 = 2.86 \times 10^3$ and $d/\delta_0 = 10$.

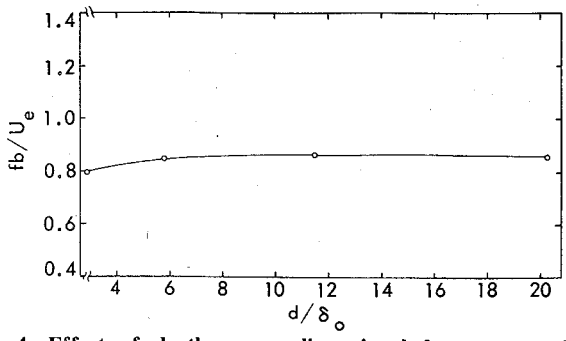

Fig. 4 Effect of depth on nondimensional frequency at $Re\delta_0 = 0.96\times10^3$ and $b/\delta_0 = 11.00$.

decreased, the cavity oscillations jumped back to the first mode where the width b/δ_0 was 8.15, and no significant hysteresis region was noticed. Beyond $b/\delta_0 > 10$, the flow over the cavity became irregular and the periodic velocity fluctuations ceased to exist or were weaker than the turbulence fluctuations in the shear layer.

Effect of Depth

Figure 4 represents the effect of depth d/δ_0 on nondimensional frequency fb/U_e at a fixed Reynolds number $Re\delta_0 = 0.96\times10^3$ and width $b/\delta_0 = 11.0$. The minimum width b_{min}/δ_0 for the onset of cavity oscillations was 9.40. The cavity began to oscillate in the second mode of oscillation with a nondimensional frequency fb/U_e of about 0.80. The results in Fig. 4 show that the nondimensional frequency was independent of depth $d/\delta_0 \geq 6$. In cavity flows with a depth d/δ_0 less than 5, nondimensional frequency dropped slowly as depth was decreased. At $d/\delta_0 = 1.34$ oscillations disappeared. Therefore, somewhere between $1.34 < d/\delta_0 < 2.87$ value of $(d/\delta_0)_{min}$ below which no cavity oscillations occur. Due to the limitations of the model, this minimum depth could not be determined precisely.

Cavity Oscillations at Different Reynolds Numbers

Figure 5 shows the results of the effect of Reynolds number $Re\delta_0$ on nondimensional frequency fb/U_e. During this experiment b/δ_0 was kept constant. Since the nondimensional frequency is independent of depth for $d/\delta_0 \geq 6$, depth d/δ_0 was not constant though care was taken not to decrease the depth below the above limit. Experimental results for three ogive nose shapes with $\ell/D = 0.6$, 1.12, and 2.12 are plotted in Fig. 5. For any particular model, shear-layer thickness at separation decreases as edge velocity increases. Therefore, to keep the nondimensional width b/δ_0 constant, the cavity width b was decreased accordingly when the edge velocity U_e was changed. Width b/δ_0 was 12.76 throughout the experiment.

Within the range of Reynolds numbers $U_e\delta_0/\nu$ tested (0.6×10^3 to 1.5×10^3), cavity oscillations occurred in the second mode of oscillation with a nondimensional frequency in the range of 0.8-0.9. Data points for different fineness ratios (ℓ/D) fall on a single curve. It was stated in the beginning of this section that nondimensional frequency fb/U_∞ is a function of $U_\infty\ell/D$, b/D, d'/D, etc. Since fb/U_e is independent of depth and, for a fixed width b/δ_0, is also independent of ℓ/D, it appears that the most appropriate parameters defining cavity oscillations are U_e and δ_0 instead of U_∞, D, and ℓ. This reduces the important nondimensional parameters of cavity oscillations by one. Hence one can conclude that nondimensional frequency fb/U_e is only a function of Reynolds number $U_e\delta_0/\nu$, depth d/δ_0, and width b/δ_0.

Mean Velocity Profile in Shear Layer

The transverse coordinate y (measured positive upward from the edge of the cavity) is nondimensionalized by the momentum thickness θ, defined as

$$\theta = \int_{-\infty}^{\infty} \frac{U}{U_e}\left(1-\frac{U}{U_e}\right)dy$$

where U_e is the velocity at the edge of the shear layer. In carrying out the above integration as one approaches inside the cavity, a cut-off was made where the mean velocity became less than 5% of the edge velocity U_e. The accuracy of measuring mean velocity by hot-wire anemometry in the vicinity of this region is very doubtful. Edge velocity U_e was almost constant along the cavity width. The mean velocity profiles at various downstream locations in nondimensional form are plotted in Fig. 6 against $(y-y_{1/2})/\theta$, where $y_{1/2}$ corresponds to $U/U_e = 0.5$. The cavity was oscillating in the first mode of oscillation with $fb/U_e = 0.67$. The downstream corner was located at $b/\theta_0 = 60$. The depth and the Reynolds number at separation were $d/\theta_0 = 100$ and $Re\theta_0 = 2.42\times10^2$.

As is clear from Fig. 6, in the early stages of shear-layer growth, the velocity profile changes from a boundary-layer profile to a shear-layer profile. A similarity has been established at $x/\theta_0 \simeq 15$. No measurements of mean-velocity profile could be made beyond $x/\theta = 50$ because of the presence of the downstream corner. Velocity fluctuations $(\overline{u'^2})^{1/2}/U_e$ as high as 0.15 were noticed in the shear layer close to the downstream corner. Results of cavity flow visualization by smoke injection, discussed later, show that these large velocity fluctuations are attributed to large lateral motion of the cavity shear layer close to the downstream corner.

To study the effect of cavity oscillations on the growth of the shear layer, mean-velocity profiles were measured for various widths b/θ_0 when edge Reynolds number $Re\theta_0 = 2.42\times10^2$ and depth $d/\theta_0 = 100$ were kept constant. From these results, the momentum thickness as defined above was computed at various downstream locations x/θ_0. Figure 7 indicates the growth of the shear layer $\theta(x)/\theta_0$ as a function of x/θ_0. Results for four cavity widths b/θ_0 equal to 52.5, 60, 85, and 105.2 were analyzed. These correspond to cavity configurations when oscillations just appeared, oscillations in the first mode, cavity flow switching between the first and second modes of oscillation, and finally the cavity in its second mode of oscillation, respectively.

It is clear from these results that the growth of the shear layer was almost linear with x/θ_0 in all modes of cavity oscillation. Growth rate $d\theta/dx$ increased in magnitude with increasing cavity widths, but no sudden jump in growth rate occurred when cavity flow switched from one mode of oscillation to another. The growth rate $d\theta/dx$, which is a measure of rate of fluid mass entrained by the growing shear layer from inside the cavity, can be studied as a function of cavity width from results shown in Fig. 7. An entrainment rate $d\theta/dx$ as low as 0.006 was observed when the cavity began to oscillate. This increased to a value as high as 0.022 for large

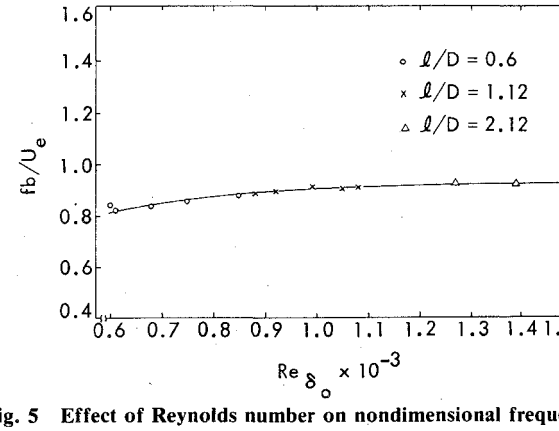

Fig. 5 Effect of Reynolds number on nondimensional frequency at $b/\delta_0 = 12.76$.

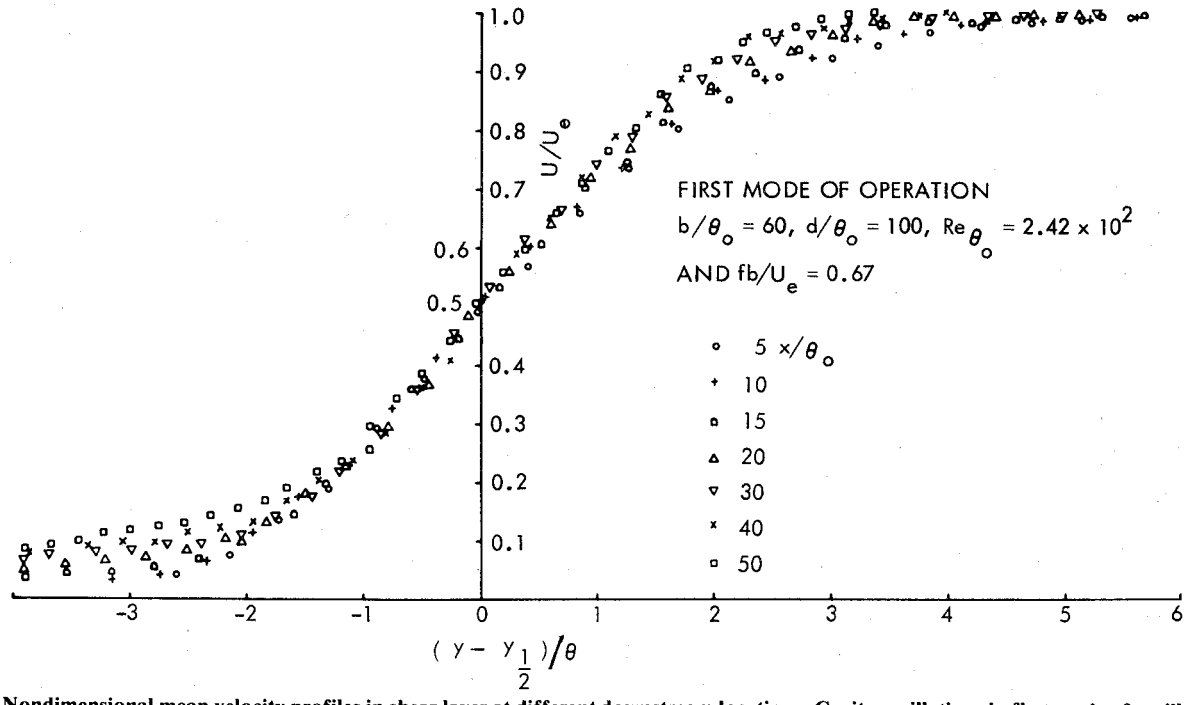

Fig. 6 Nondimensional mean velocity profiles in shear layer at different downstream locations. Cavity oscillations in first mode of oscillation with $fb/U_e = 0.67$, $b/\theta_0 = 60$, $d/\theta_0 = 100$, and $Re_{\theta 0} = 2.42 \times 10^2$.

cavity, widths when oscillations were in the second mode. Cavity oscillations are responsible for these large entrainment rates in the laminar shear layer. It should be noted that these entrainment rates are quite large for laminar shear layers and are comparable to the entrainment rate of the turbulent mixing layer, which is $d\theta/d/x \simeq 0.035$.[20]

Phase Measurements

Phase measurements of the shear-layer velocity fluctuations were made by cross-correlating the hot-wire signals at different space locations. Typical constant phase lines of the propagating disturbances relative to their phase at $x=0$ and $y=0$ at Reynolds number $Re\delta_0 = 2.86 \times 10^3$, width b/δ_0, and depth $d/\delta_0 = 10$ are shown in Fig. 8. The flow was oscillating at a frequency $f = 625$ Hz, corresponding to a nondimensional frequency $fb/U_e = 0.67$. The numbers in Fig. 8 represent the phase $\psi/2\pi$ (measured in terms of wavelength) at various space locations by which the propagating disturbances lagged behind the upstream cavity corner.

It is clear from Fig. 8 that the phase at a fixed location x/δ_0 varies a great deal across the cavity flow. As one moves toward the cavity from outside ($x/\delta_0 =$ constant), the measurements show that the phase of the disturbance decreases until one reaches the region across which a sharp drop in phase occurs. As one moves further inside the cavity, the phase of the disturbance increases. Far outside the cavity, the phase shows a linear decrease with y/δ_0, whereas far inside the measurements show a linear increase of phase.

Phase measurements of propagating disturbances through the shear layer were obtained for various cavity widths. From these measurements, the wavelengths of the disturbances were calculated. For these cavity configurations, the oscillating frequency f was known, hence the phase speed $U_c = \lambda f$ was computed. Present studies indicate that the disturbance in the shear layer propagates at a constant phase velocity, if one moves along the line where $U/U_e =$ constant. From the mean velocity and phase measurements, the phase velocity of the disturbances was computed as a function of width b/δ_0.

Results of the phase velocity U_c/U_e as a function of width b/δ_0 when the cavity was oscillating in its first and second modes of oscillation are indicated in Fig. 9. These results indicate that for a fixed depth d/δ_0 and Reynolds number $U_e \delta_0/\nu$, as width b/δ_0 was increased, the wavelength λ increased and the frequency of the disturbances dropped but the product $f\lambda = U_c$ slowly increased in magnitude. This trend was maintained until a critical value of b/δ_0 was reached when the oscillation jumped to a higher mode. This caused a sudden drop in wavelength λ of the disturbances and a sudden increase in the frequency of the oscillations. But the phase velocity of the disturbance $U_c = \lambda f$ increased steadily as the width b/δ_0 was further increased without any discontinuity as the oscillation switched modes.

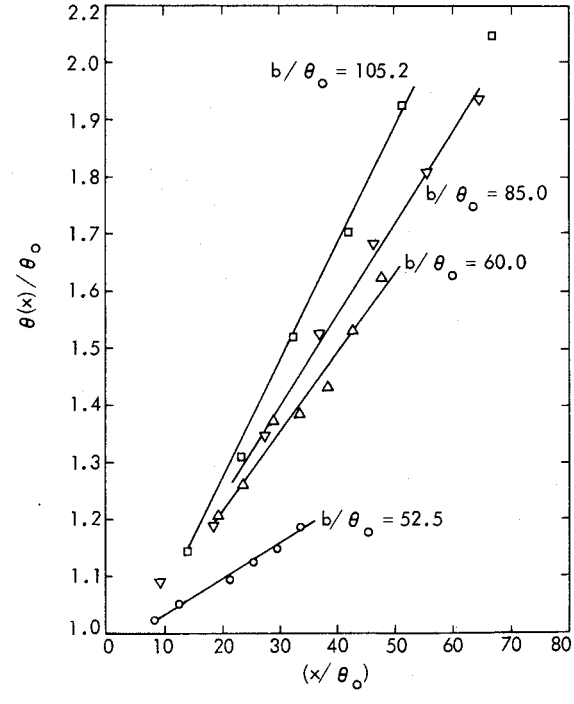

Fig. 7 Effect of cavity width on shear layer growth at $Re_{\theta 0} = 2.42 \times 10^2$ and $d/\theta_0 = 100$.

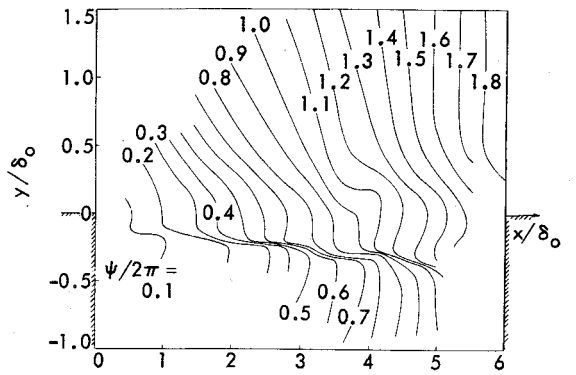

Fig. 8 Lines of constant phase in first mode of cavity oscillation at $Re\theta_0 = 2.86 \times 10^3$, $b/\delta_0 = 6$, $d/\delta_0 = 10$, and $fb/U_e = 0.67$.

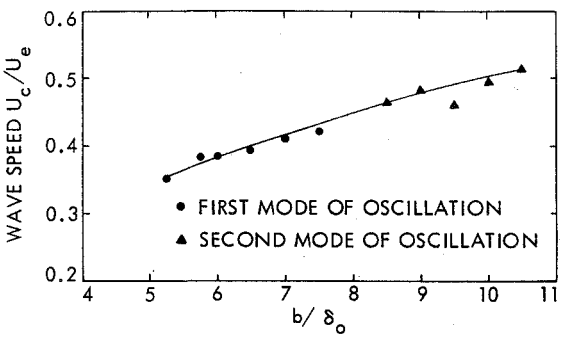

Fig. 9 Effect of width on propagation speed in the first and second modes of cavity oscillations at $Re\delta_0 = 2.86 \times 10^3$ and $d/\delta_0 = 10$.

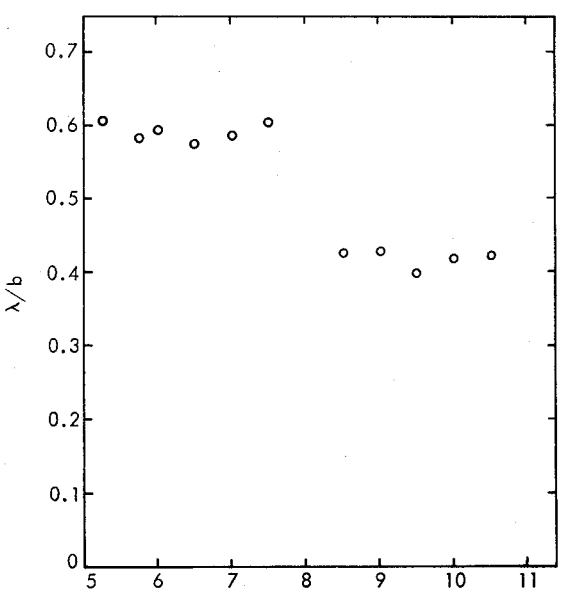

Fig. 10 Effect of cavity width on wavelength of disturbance at $Re\delta_0 = 2.86 \times 10^3$ and $d/\delta_0 = 10$.

Figure 10 shows the ratio of λ/b as a function of cavity width b/δ_0 where Reynolds number $Re\delta_0 = 2.86 \times 10^3$ and depth $d/\delta_0 = 10$ were fixed. Results for both first and second modes are shown. It should be noted that the wavelengths of the disturbances bear a nearly constant ratio to width b in any particular mode. This ratio jumps to a lower value as the cavity goes to a higher mode. This is an important experimental result, indicating that the wavelengths of the propagating disturbances have a definite integral relation to the cavity width, for each mode of cavity oscillation.

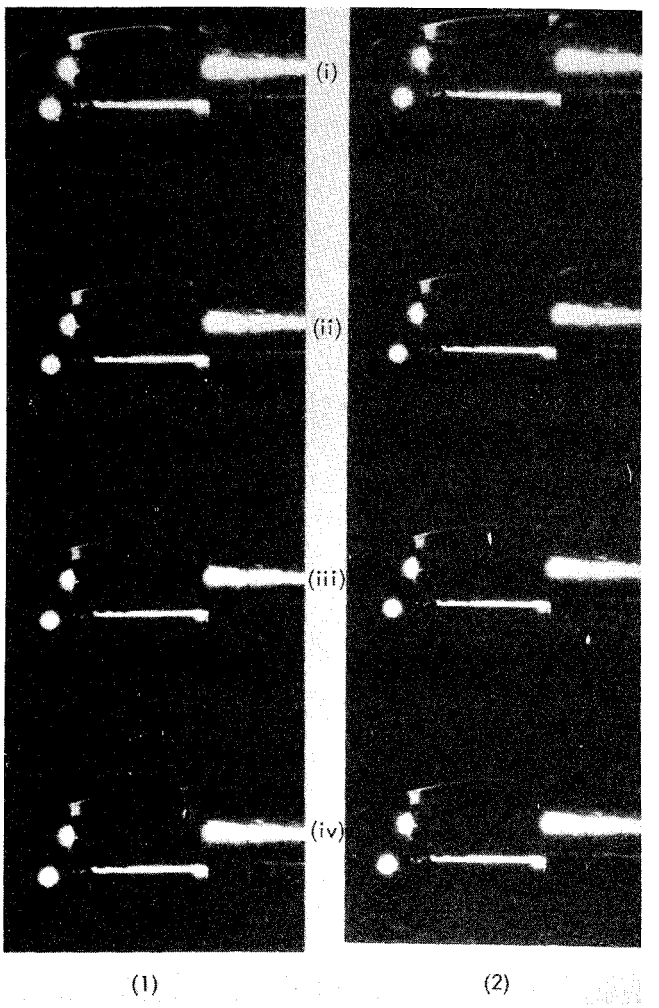

Fig. 11 Motion pictures of cavity oscillations at 500 frames/sec, $f = 300$ Hz, $b = 0.7$ in. and $d = 0.425$ in.

Flow Visualization

Figure 11 shows two sets of four consecutive frames of motion pictures taken on a 1-in.-diam model. The cavity shear layer was visualized by a continuous injection of white smoke from inside the cavity. The flow is from left to right. The freestream velocity was 30 fps with cavity width $b = 0.70$ in. and depth $d = 0.425$ in. Due to the lack of a very intense steady light source, one could only go as high as 500 frames/sec. The oscillations occurred at a frequency $f = 300$ Hz. Results of the motion pictures are summarized below:

1) Strong interaction with the downstream corner occurred when the cavity oscillations began at $b = b_{\min}$.

2) When the cavity was oscillating, the mean streakline did not oscillate much until it was very close to the downstream corner. Strong oscillations of the shear layer occurred in the vicinity of the downstream corner.

3) At the downstream corner, the mean streakline oscillated in and out at cavity oscillation frequency. As the streakline entered the cavity, the shear layer rolled up into a vortex which was shed as it deflected out of the cavity. Figure 11 a(i) shows the most inward position of the shear layer with a vortex, shed a little earlier, at the downstream corner. In Fig. 11 a(ii), the shear layer is in its most outward position and is ready to shed a vortex. The process continues at the frequency of cavity oscillations. Figure 11b shows a similar sequence of cavity oscillations.

Some Miscellaneous Observations About Cavity Flow

1) To measure the frequency of cavity oscillations, the fluctuating component of the mean velocity was analyzed. On

surveying the shear layer with the hot-wire probe, it was found that the u' fluctuations were almost sinusoidal in the shear layer except close to the downstream corner. In this region, the wave form of the u' fluctuations was quite complex. Due to rolling up of vortices in the vicinity of the downstream corner, the nonlinear effects became predominant. Higher harmonics of the fundamental frequency of cavity oscillations were noticed because of superimposed nonlinear velocity fluctuations. These higher harmonics should not be confused with the higher modes of the cavity oscillations.

2) Experiments were performed to investigate the significance of the details of the flowfield inside the cavity. The volume of the cavity was modified by inserting a thin disk inside the cavity and by adding a lip at the downstream of the cavity. These results indicate that the cavity volume does not affect the phenomenon of oscillations in flows over shallow cavitites. Therefore, the cavity oscillations based on the interaction between the shear-layer deflection and internal pressures is inadequate to explain the mechanism of oscillations in cavity flows. For more details of these experiments, the reader is advised to refer to the author's thesis.[21]

IV. Conclusion and Discussion

Minimum Cavity Width

The experimental results for laminar flow over a cavity indicate that the nondimensional width $(b_{\min}/\delta_0)\ (Re\delta_0)^{1/2}$ is independent of depth d/δ_0 for $d/\delta_0 \geq 2$. For $d/\delta_0 > 2$, the value of the width $(b_{\min}/\delta_0)\ (Re\delta_0)^{1/2}$ below which no cavity oscillations occur is 0.29×10^3. This result can be used in designing nonoscillating cavities with laminar separation. It should be noted that for a fixed edge velocity U_e and kinematic viscosity ν, minimum width $b_{\min} \sim (\delta_0)^{1/2}$. Furthermore, for laminar boundary layers without a pressure gradient, the edge velocity U_e and boundary-layer thickness at separation (for a fixed forebody shape) are related as $\delta_0 \sim 1/(U_e)^{1/2}$. Then the minimum width $b_{\min} \sim \delta_0{}^{3/2}$. It is concluded that increasing the shear-layer thickness at the upstream cavity corner tends to delay the onset of cavity oscillations.

There is a sharp increase in the nondimensional minimum width $(b_{\min}/\delta_0)\ (Re\delta_0)^{1/2}$ for $d/\delta_0 < 2$, below which no oscillations occur. Present investigation shows that the effect of decreasing cavity depth d/δ_0 is to stabilize the laminar shear flow of the cavity. It is concluded that one requires longer cavities for the onset of cavity oscillations for cavities with a smaller depth d/δ_0, compared to those with a large depth. This effect is very pronounced in very shallow cavities. In these, a strong lateral constraint on the cavity shear flow may avert the growth of three-dimensional disturbances that contribute to the transition from a laminar flow to a turbulent one.[22]

Oscillation Frequency

The overall features of cavity oscillations are given by the effect of the width b/δ_0, the depth d/δ_0 and the Reynolds number $Re\delta_0 = U_e\delta_0/\nu$, on the nondimensional frequency fb/U_e. East[2] studied oscillations in rectangular cavities with a turbulent boundary-layer separation. His results fall into two bands of frequencies fb/U_e of about 0.3 to 0.4 and others between 0.6 to 0.9 with a few results around 1.3. Similar bands of frequencies are noted in edge-tone generation.[17] Present results fall into three bands of frequencies of 0.5 to 0.6, 0.8 to 0.95, and 1.3 to 1.5. It is concluded that one gets a lower nondimensional frequency for a given mode of oscillation for a turbulent boundary-layer separation, compared to one with a laminar boundary-layer separation.

The present study shows that wavelength λ of the disturbances bears an approximate integral relation with the width $b \cong \lambda(N+1/2)$ in any particular mode of oscillation. Therefore, the nondimensional frequency can be written as $fb/U_e = (U_c/U_e)\ (N+1/2)$. Thus, an increase in the propagation speed of disturbances, with an increase of width (cf. Fig. 9) for a fixed Reynolds number, results in an increase in nondimensional frequency fb/U_e, in each mode of cavity oscillation.

Free Shear-Layer Regions

On the basis of flow visualization and hot-wire measurements of laminar cavity shear flows, one can divide cavity shear flows into the following main regions:

1) Close to the upstream cavity corner, flow transformation from a boundary layer profile to a shear layer profile occurs. Present studies indicate that this region extends as far as 10 to 15 momentum thicknesses θ_0 downstream from the point of separation.

2) The second region occupies the greater part of the cavity flow. Here pure sinusoidal velocity fluctuations of frequency f of cavity oscillations occur. This disturbance, at frequency f, propagates at a constant phase speed.

3) In this region, which lies very close to the downstream cavity corner, the shear layer deflects in and out of the cavity at the frequency f of cavity oscillations. This gross lateral motion of the shear layer causes large velocity fluctuations and results in a periodic shedding of vortices at a frequency f from the downstream corner.

Mean and fluctuating velocity measurements further show that the effect of the downstream cavity corner on cavity shear flow is to postpone the separated laminar layer to turbulence. The experiments show that the cavity shear layer remains laminar until a maximum width $b_{\max}$ is reached. At $b_{\max}$, the periodic signal could not be measured due to increased turbulence over a range of Reynolds number at separation $Re\delta_0 = 5\times10^2$ to 2×10^3. A maximum width $b_{\max}/\theta_0 \gtrsim 100$ was observed. This width is nearly twice as large as the distance of transition from separation of laminar shear layer.[23] The stabilizing effect may be attributed to these large self-sustained oscillations induced in the cavity shear layer by the presence of the downstream corner. Presence of these oscillations seems to delay the rolling up of the laminar shear layer into vortices.

The experiments show that the presence of cavity oscillations in the flow induces a large increase in the shear-layer growth rate. These large growth rates may be caused by increased "Reynolds stress" $\overline{u'v'}$ due to the presence of large amplitude oscillations in the cavity shear layer.

Summary and Conclusions

1) The phenomenon of oscillations in low-speed flows over cavities is not an acoustic resonance phenomenon in the longitudinal direction. These oscillations result from propagating disturbances which get amplified along the cavity shear layer.

2) The present experiments show that the onset of cavity oscillations is accompanied by a large lateral motion of the cavity shear layer close to the downstream corner. This also results in periodic shedding of the vortices from the downstream corner at the frequency of cavity oscillations.

3) It is further observed that the transition of the laminar cavity shear flow to turbulence is postponed by the presence of large amplitude oscillations in cavity flow until a maximum width $b_{\max}$ is reached. No rolling up of the laminar cavity shear layer into vortices occurs for cavity widths as large as $b/\theta_0 > 100$. The transition phenomenon which occurs for widths $b > b_{\max}$ is quite complex and needs further experimental investigation.

4) It is observed that the effect of depth for $d/\delta_0 \sim O(1)$ is to delay the transition of the free laminar shear-layer flow to a turbulent one.

5) The presence of strong cavity oscillations contributes to a large growth of the shear layer. Growth rates $d\theta/dx \simeq 0.022$ in laminar cavity flows are noticed.

6) The results show that for shallow cavities, an approximate integral relation between the wavelength of the propagating disturbance λ of the cavity oscillations and width b given by $b/\lambda \simeq (n+1/2)$ exists, where n can be 0, 1, 2, 3, ... etc., depending upon the mode of cavity oscillation.

7) Cavity volume does not affect the phenomenon of oscillations in flows over shallow cavities.

Acknowledgments

The financial support provided by the U.S. Army Research Office through Contract No. DAHC-04-72-C-0028, which made these experiments possible, is gratefully acknowledged. Gratitude is extended to Professors T. Kubota and A. Roshko for their valuable guidance throughout this work. The author also gives his sincere appreciation to Dr. W. Behrens for his helpful suggestions.

References

[1] Charwat, A. F., Roos, J. N., Dewey, F. C., and Hitz, J. A., "An Investigation of Separated Flows. Part 1. The Pressure Field," *Journal of the Aerospace Sciences*, Vol. 28, June 1961, pp. 457-470.

[2] East, L. F., "Aerodynamic Induced Resonance in Rectangular Cavities," *Journal of Sound and Vibrations*, Vol. 3, March 1966, pp. 277-287.

[3] Plumblee, H. E., Gibson, J. S., and Lassiter, L. W., "A Theoretical and Experimental Investigation of the Acoustic Response of Cavities in an Aerodynamic Flow," WADD-TR-61-75, March 1962.

[4] Tani, I., Iuchi, M., and Komoda, H., "Experimental Investigation of Flow Separation Associated with a Step or a Groove," Aero Research Institute, Univ. of Tokyo Rept. No. 364, April 1961.

[5] Boeing Airplane Co., "Investing of B-47 Bomb Bay Buffeting," Rept. D-12675, Feb. 15, 1952.

[6] Brazier, J. G., "The Hydrostatic Channel and A3D-1 Bomb Bay Buffering Tests," Douglas Aircraft Co. Report No. ES 17825, Dec. 27, 1954.

[7] Rossiter, J. E. and Kurn, A. G., "Wind Tunnel Measurement of Unsteady Pressures in and Behind a Bomb Bay," (Canberra) A.R.C.C.P. 728, Oct. 1962.

[8] Karamcheti, K., "Sound Radiated from Surface Cutouts in High-Speed Flows," Ph.D. Thesis, California Institute of Technology, June 1956.

[9] Heller, H. H., Holmes, D. G., and Covert, E. E., "Flow Induced Pressure Oscillations in Shallow Cavities," *Journal of Sound and Vibrations*, Vol. 18, No. 4, 1971, pp. 545-552.

[10] McGregor, W. and White, R. A., "Drag of Rectangular Cavities in Supersonic and Transonic Flows Including the Effects of Cavity Resonance," *AIAA Journal*, Vol. 8, Nov. 1970, pp. 1959-1964.

[11] Rossiter, J. E., "Wind Tunnel Experiments on the Flow Over Rectangular Cavities at Subsonic and Transonic Speeds," communicated by the Deputy Controller Aircraft (Research and Development) Ministry of Aviation, R&M No. 3438, Oct. 1964. (Replace R.A.E. Tech. Rept. No. 64037-A.R.C. 26621).

[12] Bilanin, A. J. and Covert, E. E., "Estimation of Possible Excitation Frequencies for Shallow Rectangular Cavities," *AIAA Journal*, Vol. 11, March 1973, pp. 347-351.

[13] Roshko, A., "Some Measurements of Flow in a Rectangular Cutout," NACA TN-3488, 1955.

[14] Spee, B. M., "Wind Tunnel Experiments on Flow over Rectangular Cavities at Subsonic and Transonic Speeds," *AGARD Conference Proceedings No. 4*, Separated Flows, Pt. 2, 1966.

[15] Stull, F. C., Curran, E. T., and Velkoff, H. R., "Investigation of Two-Dimensional Cavity Diffusers," AIAA Paper No. 73-685, AIAA 6th Fluid and Plasma Dynamic Conference, Palm Springs, California, July 1973.

[16] Woolley, J. P., and Karamcheti, K.,"A Study of Narrow Band Noise Generation by Flow Over Ventilated Walls in Transonic Wind Tunnels," Nielsen Engineering and Research, Inc. (NEAR) TR 50, Feb. 1973.

[17] Karamcheti, K. and Bauer, A. B., "Edgetone Generation," Stanford University, Dept. of Aero. and Astro., Rept. SUDDAR 162, July 1963.

[18] Shields, W. L. and Karamcheti, K., "An Experimental Investigation of the Edgetone Flow Field," Stanford Univ., Dept. of Aero. and Astro., Rept. SUDDAR 303, Feb. 1967.

[19] Stegan, G. R. and Karamcheti, K., "On the Structure of an Edgetone Flowfield," Stanford Univ., Dept. of Aeronautics and Astronautics, Rept. SUDDAR 303, Feb. 1967.

[20] Liepmann, H. W. and Lufer, J., "Investigation of Free Turbulent Mixing," NACA Tech. Note No. 1257, 1947.

[21] Sarohia, V., "Experimental and Analytical Investigation of Oscillations in Flows Over Cavities," Ph.D. Thesis, Dept. of Aeronautics, California Institute of Technology, Pasadena, Calif., March 1975.

[22] Roshko, A., "Transition in Incompressible Near-Wakes," *The Physics of Fluids*, Suppl., 1967.

[23] Sato, H., "Experimental Investigation of the Transition of Laminar Separated Layer," *Journal of the Physical Society of Japan*, Vol. 11, June 1956, pp. 702-709.